Effects of nanocrystal shape and size on the temperature sensitivity in Raman thermometry

Liangliang Chen, Kelly Rickey, Qing Zhao, Christopher Robinson, and Xiulin Ruan[a)]
School of Mechanical Engineering and Birck Nanotechnology Center, Purdue University, West Lafayette, Indiana 47907, USA

(Received 16 April 2013; accepted 8 August 2013; published online 20 August 2013)

The effects of CdSe nanocrystal (NC) shape and size on the temperature sensitivity of the Raman shift have been investigated, for the interest of Raman thermometry using NCs. For spherical CdSe NCs of diameters 2.8 nm, 3.6 nm, and 4.4 nm, the temperature sensitivities are $-0.0131\,cm^{-1}/K$, $-0.0171\,cm^{-1}/K$, and $-0.0242\,cm^{-1}/K$, respectively. This trend indicates that as the diameter increases, the effect of increasing phonon anharmonicity dominates over the effect of the decreasing thermal expansion coefficient. On the other hand, triangular NCs with a size of 4.2 nm and elongated NCs of a dimension of 4.6 nm by 14 nm show temperature sensitivities of $-0.0182\,cm^{-1}/K$ and $-0.0176\,cm^{-1}/K$, respectively. This trend indicates that in non-spherical shape NCs, the effect of decreasing thermal expansion coefficient dominates over the effect of slightly increasing phonon anharmonicity. The selection of NCs for Raman thermometry should depend on the specific requirements of temperature sensitivity, spatial resolution, and response time. © *2013 AIP Publishing LLC*. [http://dx.doi.org/10.1063/1.4819170]

Raman spectroscopy has been widely used to characterize phonon properties of bulk materials and nanostructures. Due to the dependence of Raman shift, intensity, and linewidth on temperature, recently Raman spectroscopy has also been actively used for thermometry.[1–3] Raman thermometry has the benefits such as non-contact technique and easy preparation of samples. For thermometry applications, high temperature sensitivity, high spatial resolution, and fast response are usually desired. When nanocrystals are used in Raman thermometry, high spatial resolution and fast response can be readily achieved due to the extremely small size of nano crystals. However, the temperature sensitivity is generally low due to the small Raman shift as a function of temperature for most materials. For example, the temperature sensitivity of the Raman shift in graphene and silicon are $-0.016\,cm^{-1}/K$ (Ref. 1) and $-0.022\,cm^{-1}/K$ (Ref. 3), respectively, yielding a practical temperature resolution of 1–2 K in Raman thermometry.

On the other hand, semiconductor nanocrystals can be synthesized with different sizes and shapes, which can significantly affect their Raman properties. This provides an additional dimension to tune and potentially enhance the temperature sensitivity in Raman thermometry. Also, their compatibility with solvent/solutions makes them particularly suitable for temperature sensing in biological or chemical environments.[4] Tanaka *et al.* found that the LO phonon peak of CdSe nanocrystals (NCs) shifted to lower frequencies and the linewidth broadened with decreasing NC size or increasing temperature.[5] Meulenberg *et al.* investigated CdSe-core ZnS-shell nanocrystal and showed that the ZnS-shell-induced LO phonon shift was larger for smaller dots than for larger dots because of the larger compressive stress resulting from the larger mismatch between core and shell for smaller dots.[6] Kusch *et al.* found that higher-order phonon processes were enhanced with decreasing NC size.[7] However, little work has been performed to study the combined shape and size effect on temperature sensitivity due to the challenge of synthesizing monodisperse nanocrystals.

Here we report the effects of nanocrystal shape and size on the temperature sensitivity in Raman thermometry, using CdSe nanocrystals as the model material. This is made possible by recent progress in the synthesis of monodisperse CdSe NCs of various shapes.[8–10] We prepared CdSe nanocrystals with precise shape and size control, followed by a systematic measurement of their temperature-dependent Raman spectra. We then fitted the experimental data to a linear model to gain a deeper insight into how the geometry influenced the relation between the Raman shift and temperature. Discussions on the selection of nanocrystals for Raman thermometry are given at the end.

Unless stated otherwise, all chemical reagents were purchased from Alfa Aesar. In this work, CdSe NCs were synthesized using the method of organometallic compound pyrolysis,[8,11] commonly used to prepare highly crystalline monodisperse CdSe NCs by employing a hot-injection technique for a fast-nucleation process. A typical synthesis involved three main steps: preparation of the selenium precursor, preparation of the cadmium precursor, and injection and growth.

To prepare the selenium precursor, 0.1262 g selenium (Se) and 3 ml tri-n-octylphosphine (TOP) were loaded into a flask and then heated up to 150 °C. After the solution turned clear, it was removed from the heater and then transferred into a syringe for injection after cooling to room temperature. To prepare the cadmium precursor, cadmium oxide (CdO), surfactants, and solvent were loaded into a flask, heated to 300 °C, and maintained at this temperature until the solution turned clear. For spherical NCs, 0.2054 g CdO, 0.4508 g tetradecylphosphonic acid (TDPA), 10 ml oleic acid (OA), and 10 ml 1-octadecene (ODE) were used. For triangular NCs,

a)ruan@purdue.edu

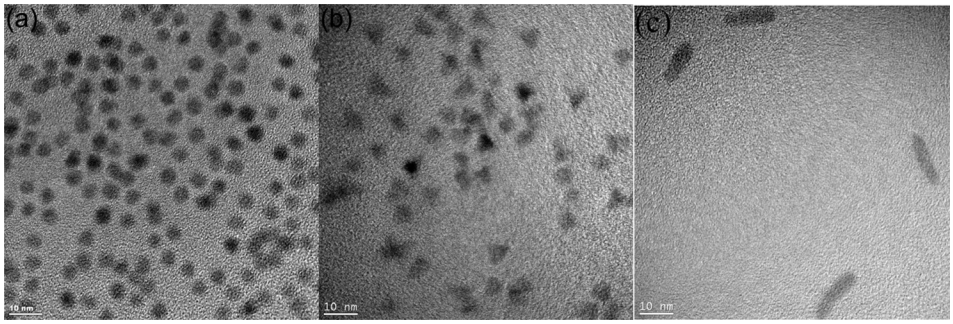

FIG. 1. Typical TEM images. (a) Sample 3; (b) sample 4; (c) sample 5.

0.2054 g CdO, 0.4508 g TDPA, and 3.2751 g tri-n-octylphosphine oxide (TOPO) were used. For elongated NCs, 0.2054 g CdO, 0.4508 g TDPA, 0.2741 g hexylphosphonic acid (HPA), and 3.2751 g TOPO were used. To grow NCs, the Se precursor was quickly injected into the Cd precursor solution with vigorous stirring at 300 °C, and the solution was maintained at this temperature for various durations. Generally, longer reaction times resulted in larger NCs. After the reaction was performed, the hot solution was immediately quenched with a mixture of ice and water. The as-prepared NCs were thoroughly cleaned by repeating the cycle of precipitation and dissolution six times. Hexanes and ethanol were used as the solvent/non-solvent couple.

Two series of CdSe NCs have been synthesized: spherical NCs of different diameters and NCs of similar diameter but different shapes. Samples 1, 2, and 3 are in the category of spherical NCs with a diameter of 2.8 nm, 3.6 nm, and 4.4 nm, respectively. Samples 3, 4, and 5 are in the category of NCs of similar diameter but different shapes: Sample 3 has a spherical shape with a diameter of 4.4 nm; sample 4 has a triangular shape with a size of 4.2 nm; and sample 5 has an elongated shape with a diameter of 4 nm and a length of 14 nm.

For UV-Vis absorption spectroscopy, the samples were prepared by dispersing the NCs into hexanes, and the absorption spectra were recorded on SpectraMax Plus 384 plate reader with a spectral resolution of 1 nm. The samples for TEM were prepared by dropping the hexanes solution onto copper grids coated with holey carbon films, and the TEM images were obtained on an FEI-Tecnai TEM with an accelerating voltage of 200 kV. Samples for Raman spectroscopy were prepared by dropping the solution onto glass slides to form closely-packed films, and Raman spectra were recorded on Jobin-Yvon T64000 high resolution Raman spectrometer with an excitation energy of 2.33 eV (532 nm) and a laser power of ~0.2 mW.

Figures 1(a)–1(c) show typical TEM images of the spherical, triangular, and elongated NCs, respectively. For the spherical samples, the diameter varies up to ±0.2 nm. For the triangular samples, the diameter varies up to ±0.4 nm. For the elongated samples, the diameter and length vary up to ±0.2 nm and ±1.2 nm, respectively. The monodispersity in size and shape ensures that the influence of size and shape distribution on Raman spectra is minimized.

The UV-Vis absorption spectroscopy is used to monitor the size evolution and distribution of all the samples during the temperature-dependent Raman measurements. Figure 2 shows the typical absorption spectra obtained before and after the Raman experiments. For the purpose of clarification, a vertical line is drawn to mark the peak position of the first excitonic transition ($1S_e$ and $1S_h$). It can be seen that no obvious change in peak position or width has occurred after the Raman experiments, indicating no surface environment change or NC growth induced by local-heating. This can be attributed to the low excitation-laser power and the protection of residual OA and TOPO from oxidization (both OA and TOPO are strong binding ligands,[12] unlike pyridine).

Figure 3 shows the Raman spectra as a function of temperature for all the five CdSe samples. For the purpose of clarification, the spectra are normalized to the intensity of the LO phonon peaks and then shifted vertically. The spectral resolution is 0.0195 cm^{-1}. It is seen that for each sample the LO phonon peak shifts to lower frequencies and broadens with increasing temperature, which can be attributed to the anharmonicity in the inter-atomic potential.[5,7,13] The broad surface mode has been suppressed significantly, which can be attributed to the modified dielectric medium in the closely packed NC assemblies.[14]

As suggested by Burke *et al.*,[15] the Raman frequency can be written as a function of temperature as

$$\omega(T) = \omega_0 + \Delta\omega_{TE}(T) + \Delta\omega_A(T), \quad (1)$$

where ω_0, $\Delta\omega_{TE}(T)$, and $\Delta\omega_A(T)$ represent the frequency at 0 K, the frequency shift due to thermal expansion effect, and the frequency shift due to anharmonic phonon-phonon interaction, respectively. A high thermal expansion coefficient and a strong anharmonic phonon process can both lead to higher Raman shift. Within the temperature range studied in

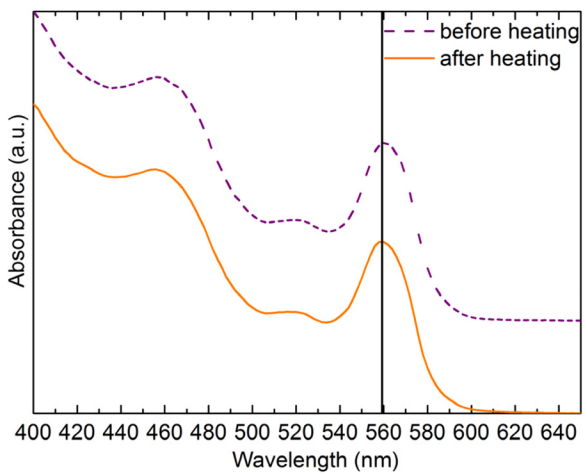

FIG. 2. Typical UV-Vis spectra obtained before and after the Raman experiments.

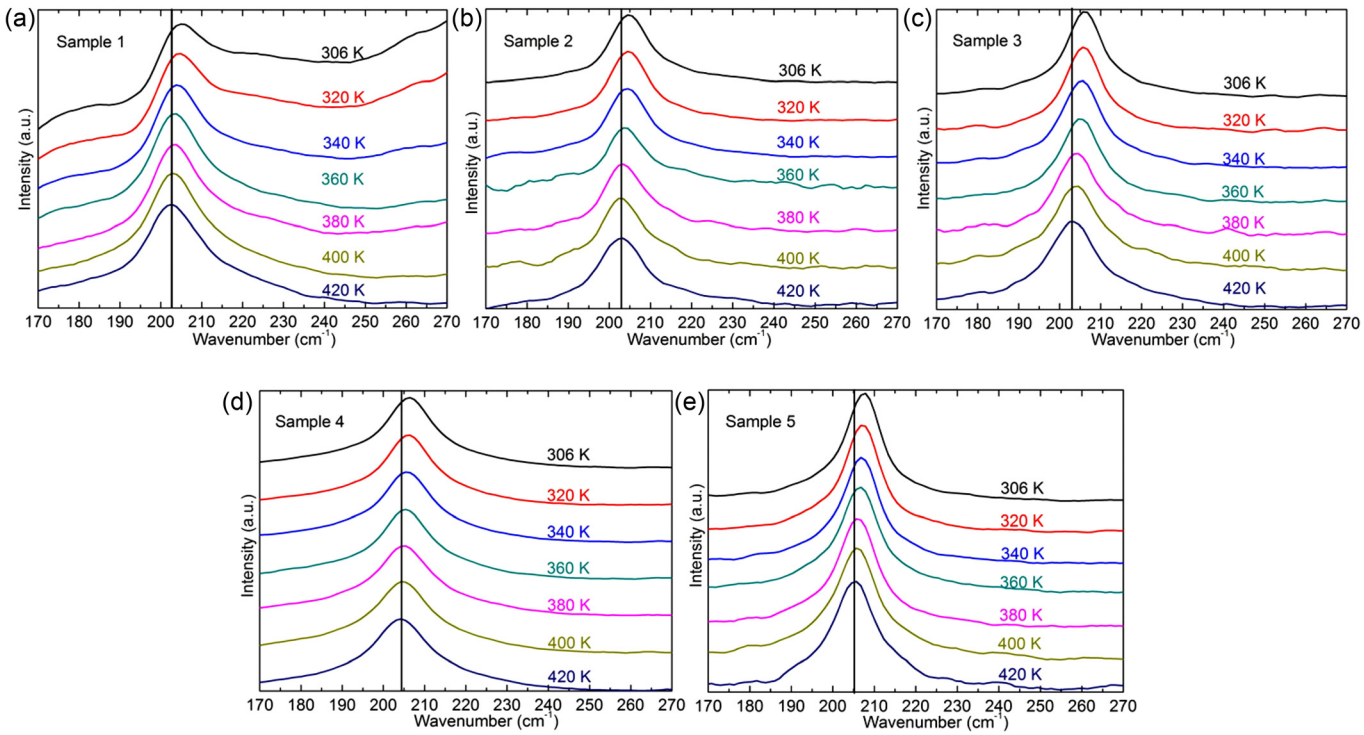

FIG. 3. Raman spectra for five different samples from 306 K to 420 K. (a) Sample 1; (b) sample 2; (c) sample 3; (d) sample 4; (e) sample 5.

this work (300 K–420 K), both $\Delta\omega_{TE}(T)$ (Ref. 13) and $\Delta\omega_A(T)$ (Ref. 16) can be approximated to change linearly with temperature. Therefore, the overall frequency shift varies linearly with temperature and can be approximated as[15]

$$\Delta\omega(T) \approx -3\omega_0\alpha\gamma\Delta T - 4\frac{k}{hc\omega_0}$$
$$a\Delta T = -\left(3\omega_0\alpha\gamma + 4\frac{k}{hc\omega_0}a\right)\Delta T, \qquad (2)$$

where α, γ, a, k, h, and c represent the linear thermal expansion coefficient, the Gruneisen parameter, the constant for the anharmonic three-phonon process, the Boltzmann constant, the Planck constant, and the speed of light in vacuum, respectively.

The peak frequency is extracted from the Raman spectra by fitting the peak profile with a Lorentzian function. Figure 4 shows the LO phonon peak frequency as a function of temperature for two series of NC samples. At any temperature, the Raman shift is higher for larger NC diameter, consistent with previous studies.[17] The data points can be well fitted with the linear model, and the fitting results are inset in the figures. Figure 4(a) shows the results for spherical NCs of different diameters. It is seen that the temperature sensitivities are $-0.0131\,\mathrm{cm}^{-1}/\mathrm{K}$, $-0.0171\,\mathrm{cm}^{-1}/\mathrm{K}$, and $-0.0242\,\mathrm{cm}^{-1}/\mathrm{K}$ for diameters of 2.8 nm, 3.6 nm, and 4.4 nm, respectively. These results indicate higher temperature sensitivity in larger NCs. To explain this trend, we notice that the linear thermal expansion coefficient decreases with increasing size,[18] but the constant for the anharmonic three-phonon process can increase with increasing size.[7] Overall, as the diameter of our NCs increases, the effect of increasing anharmonic phonon process dominates over the effect of decreasing thermal expansion coefficient, giving higher temperature sensitivity in larger NCs.

Figure 4(b) shows the temperature sensitivity for NC samples of similar diameter but different shapes. This series of samples were designed to study the effect of shape while minimizing the effect of diameter. At room temperature, the Raman shift of the elongated sample is higher than that of the spherical and triangular samples, probably due to the larger size. The temperature sensitivity for the triangular NC sample is $-0.0182\,\mathrm{cm}^{-1}/\mathrm{K}$, which is lower than that of the

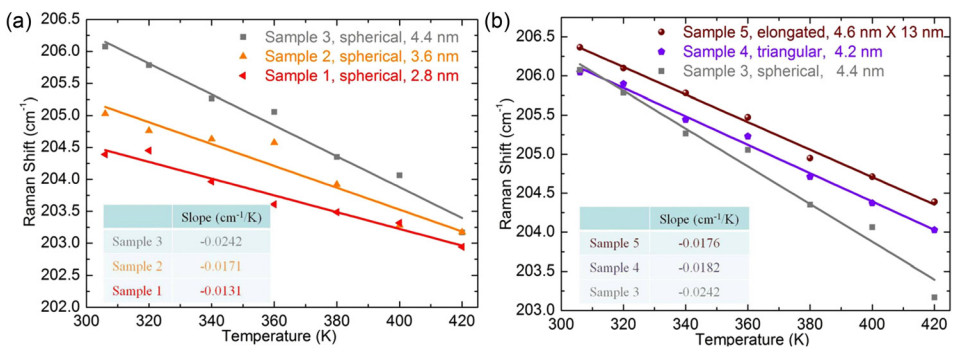

FIG. 4. The LO phonon frequency as a function of temperature. (a) Spherical CdSe NCs of different sizes; (b) various-shaped CdSe NCs of similar size.

spherical NC sample. This may be partially explained by the slightly smaller size (4.2 nm) of the triangular NCs than that of the spherical NCs (4.4 nm). However, if we interpolate the data in Figure 4(a), we would get a temperature sensitivity of $-0.0224\,cm^{-1}/K$ for spherical NCs with a diameter of 4.2 nm, indicating that the triangular shape contributes more to the reduction of temperature sensitivity. Similarly, the temperature sensitivity of the elongated NCs of a diameter 4.6 nm is $-0.0176\,cm^{-1}/K$, which is lower than that of the spherical NCs of the diameter 4.4 nm, even if the diameter of the former is larger. An extrapolation of the data in Figure 4(a) would give a temperature sensitivity of $-0.0260\,cm^{-1}/K$ for spherical NCs with a diameter of 4.6 nm, indicating that the significantly reduced temperature sensitivity is mainly due to the elongated shape. It has been shown that the elongated CdSe NCs are grown from the spherical NCs along the c-axis[10] and the LO phonon vibrates along the c-axis.[19] This indicates the necessity to take into account the thermal expansion effect in explaining our trend. The dimension along the c-axis is much larger in the elongated NCs than in the spherical NCs, which can result in a much smaller linear thermal expansion coefficient[18] in the elongated NCs. According to Eq. (2), our trend indicates that the effect of the reduced thermal expansion coefficient dominates over the effect of the slightly increased anharmonic effect in elongated NCs. Hence, the overall effect is to reduce the temperature sensitivity in elongated NCs than in spherical NCs.

Based on the above results, we can see that the temperature sensitivity of spherical nanocrystals increases with increasing size. However, smaller nanocrystals could give higher spatial resolution. For the same diameter, spherical nanocrystals show higher temperature sensitivity than other shapes. However, non-spherical nanocrystals may be preferred in certain applications. The selection of nanocrystals for Raman thermometry should depend on the requirements for the specific applications.

By using the method of organometallic compound pyrolysis, highly crystalline 0D and 1D CdSe NCs have been synthesized. Raman spectroscopy is used to study how the NC shape and size affect the temperature sensitivity of the Raman shift corresponding to the LO phonon. For spherical CdSe NCs of diameters 2.8 nm, 3.6 nm, and 4.4 nm, the temperature sensitivities are $-0.0131\,cm^{-1}/K$, $-0.0171\,cm^{-1}/K$, and $-0.0242\,cm^{-1}/K$, respectively. This trend indicates that as the diameter increases, the effect of increasing phonon anharmonicity dominates over the effect of the decreasing thermal expansion coefficient. Although larger NCs show higher temperature sensitivity, smaller NCs could give a higher spatial resolution. On the other hand, triangular NCs with a size of 4.2 nm and elongated NCs of a dimension of 4.6 nm by 14 nm show temperature sensitivities of $-0.0182\,cm^{-1}/K$ and $-0.0176\,cm^{-1}/K$, respectively. This trend indicates that in non-spherical shape NCs, the effect of decreasing thermal expansion coefficient dominates over the effect of slightly increasing phonon anharmonicity. Such information is useful in the selection of NCs to tune temperature sensitivity, spatial resolution, and time constant for specific applications.

This work is partially supported by NSF grant (No. CTS-0933559) and NSF CAREER Award (No. CBET-1150948). Useful discussions with Dr. Sarpangala Venkataprasad Bhat are gratefully appreciated.

[1]A. A. Balandin, S. Ghosh, W. Z. Bao, I. Calizo, D. Teweldebrhan, F. Miao, and C. N. Lau, Nano Lett. **8**(3), 902 (2008); J. H. Seol, I. Jo, A. L. Moore, L. Lindsay, Z. H. Aitken, M. T. Pettes, X. S. Li, Z. Yao, R. Huang, D. Broido, N. Mingo, R. S. Ruoff, and L. Shi, Science **328**(5975), 213 (2010).
[2]L. Song, W. J. Ma, Y. Ren, W. Y. Zhou, S. S. Xie, P. H. Tan, and L. F. Sun, Appl. Phys. Lett. **92**(12), 121905 (2008); S. H. Kim, J. Noh, M. K. Jeon, K. W. Kim, L. P. Lee, and S. I. Woo, J. Micromech. Microeng. **16**(3), 526 (2006); L. M. Phinney, J. R. Serrano, E. S. Piekos, J. R. Torczynski, M. A. Gallis, and A. D. Gorby, J. Heat Transfer **132**(7), 072402 (2010); J. R. Serrano and S. P. Kearney, J. Heat Transfer **130**(12), 122401 (2008); J. D. Smith, C. D. Cappa, W. S. Drisdell, R. C. Cohen, and R. J. Saykally, J. Am. Chem. Soc. **128**(39), 12892 (2006).
[3]X. D. Tang, Y. N. Yue, X. W. Chen, and X. W. Wang, Opt. Express **20**(13), 14152 (2012).
[4]S. Singh, K. Bozhilov, A. Mulchandani, N. Myung, and W. Chen, Chem. Commun. **46**(9), 1473 (2010).
[5]A. Tanaka, S. Onari, and T. Arai, Phys. Rev. B **45**(12), 6587 (1992).
[6]R. W. Meulenburg, T. Jennings, and G. F. Strouse, Phys. Rev. B **70**(23), 235311 (2004).
[7]P. Kusch, H. Lange, M. Artemyev, and C. Thomsen, Solid State Commun. **151**(1), 67 (2011).
[8]C. B. Murray, D. J. Norris, and M. G. Bawendi, J. Am. Chem. Soc. **115**(19), 8706 (1993); F. Shieh, A. E. Saunders, and B. A. Korgel, J. Phys. Chem. B **109**(18), 8538 (2005).
[9]X. G. Peng, L. Manna, W. D. Yang, J. Wickham, E. Scher, A. Kadavanich, and A. P. Alivisatos, Nature **404**(6773), 59 (2000).
[10]L. Manna, E. C. Scher, and A. P. Alivisatos, J. Am. Chem. Soc. **122**(51), 12700 (2000).
[11]W. Wang, S. Banerjee, S. G. Jia, M. L. Steigerwald, and I. P. Herman, Chem. Mater. **19**(10), 2573 (2007).
[12]I. Lokteva, N. Radychev, F. Witt, H. Borchert, J. Parisi, and J. Kolny-Olesiak, J. Phys. Chem. C **114**(29), 12784 (2010).
[13]G. Doerk, C. Carraro, and R. Maboudian, Phys. Rev. B **80**(7), 073306 (2009).
[14]Y. N. Hwang, S. H. Park, and D. Kim, Phys. Rev. B **59**(11), 7285 (1999).
[15]H. Burke and I. Herman, Phys. Rev. B **48**(20), 15016 (1993).
[16]M. Balkanski, R. Wallis, and E. Haro, Phys. Rev. B **28**(4), 1928 (1983).
[17]H. Lange, M. Artemyev, U. Woggon, and C. Thomsen, Nanotechnology **20**(4), 045705 (2009).
[18]K. Lu and M. L. Sui, Acta Metall. Mater. **43**(9), 3325 (1995).
[19]Y. N. Hwang, S. H. Shin, H. L. Park, S. H. Park, U. Kim, H. S. Jeong, E. J. Shin, and D. Kim, Phys. Rev. B **54**(21), 15120 (1996).